Highly Flexible Dielectric Films from Solution Processable Covalent Organic Frameworks

Milinda C. Senarathna[†1], He Li[†2,3], Sachini D. Perera[1], Jose Torres-Correas[1], Shashini D. Diwakara[1], Samuel R. Boardman[1], Yi Liu[2,3]*, Ronald A. Smaldone[1]*

[1] Department of Chemistry and Biochemistry, University of Texas at Dallas, 800 West Campbell Road, Richardson, Texas, 75080, United States.

[2] The Molecular Foundry, Lawrence Berkeley National Laboratory, Berkeley, California, 94720, United States.

[3] Materials Sciences Division, Lawrence Berkeley National Laboratory, Berkeley, California, 94720, United States.

KEYWORDS: Covalent organic frameworks, film fabrication, dielectrics, dynamic covalent chemistry, mechanical characterization

Summary

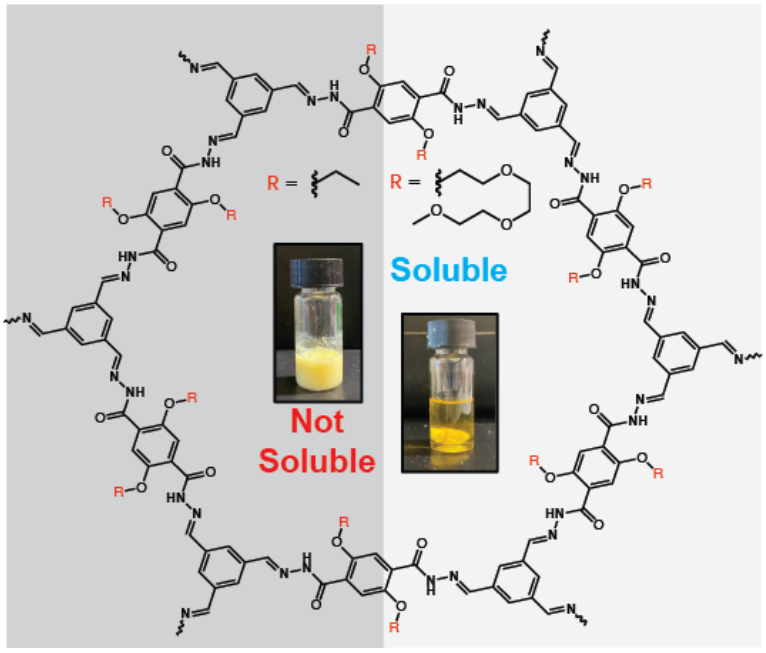

Covalent organic frameworks (COFs) are known to be a promising class of materials for a wide range of applications, yet their poor solution processability limits their utility in many areas. Here we report a pore engineering method using hydrophilic side chains to improve the processability of hydrazone and β-ketoenamine-linked COFs and the production of flexible, crystalline films. Mechanical measurements of the free-standing COF films of COF-PEO-3 (hydrazone-linked) and TFP-PEO-3 (β-ketoenamine-linked), revealed a Young's modulus of 391.7 MPa and 1034.7 MPa, respectively. The solubility and excellent mechanical properties enabled the use of these COFs in dielectric devices. Specifically, the TFP-PEO-3 film-based dielectric capacitors display simultaneously high dielectric constant and breakdown strength, resulting in a discharged energy density of 11.22 J cm^{-3}. This work offers a general approach for producing solution processable COFs and mechanically flexible COF-based films, which hold great potential for use in energy storage and flexible electronics applications.

Introduction

Since the initial discovery of covalent organic frameworks (COFs) in 2005,[1] they have evolved into a promising class of materials for applications in energy storage,[2] molecular separation,[3,4] and heterogeneous catalysis,[5] due to their crystallinity, high surface area, and wide scope of functionality. While the permanent porosity of COFs has drawn the

most attention for application development, two-dimensional (2D) COFs have recently gained interest for use in other types of applications such as dielectric devices[6,7] and ballistic materials,[8,9,10,11,12] where other types of 2D materials (*e.g.,* graphene[13]) have often been a focus. While most classes of 2D materials face challenges in their synthesis and scalability,[14] 2D COFs can be produced as highly crystalline polymers, even in bulk quantities.[15,16] Though all these reports show that COFs have significant potential, one of the main limitations of these polymers is that their powder forms demonstrate poor solubility and processability in most common solvents.[17,18] This limits the potential of COFs for use in practical applications where traditional plastics are used because they cannot be molded or shaped.

Despite these challenges, several COF processing methods have been developed to address this key issue. These methods have allowed some COFs to be processed into useful thin films,[3,6,19,20] composites,[21,22] nanotubes,[23,24] and gels[25,26] either *via* post-synthetic processing of COF powders (top-down approach) or directly synthesizing them from monomers (bottom-up approach) (Figure 1).

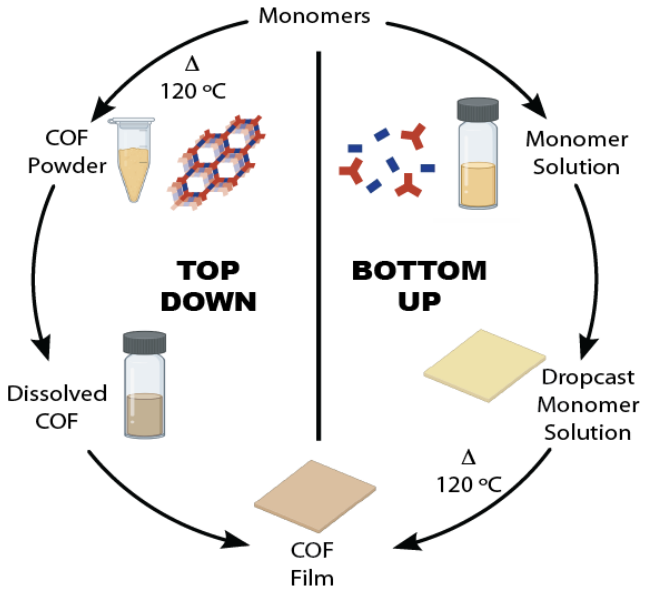

Figure 1. Illustration of the COF film fabrication processes described in this work. The "top-down" method involves synthesizing a COF powder using conventional solvothermal conditions, followed by solution casting and drying. The "bottom-up" procedure casts the film from a solution of monomer precursors and subjects the resulting film to conventional solvothermal conditions to produce the COF film *in situ*.

Among these processed materials, films and membranes are important due to their potential usage in many fabricated electrical or mechanical devices.[27] There are several techniques to fabricate COF films using a bottom-up approach.[28,29] Some of the major limitations of this approach involve the scalability of the synthesis, lack of general compatibility with different COF compositions, and lack of control over the film thickness. Top-down synthesis methods involve techniques such as sonication,[30] mechanical grinding,[31] compression[32] and solution casting[17] to shape 2D COFs into thin films and membranes.

While reliable top-down methods to produce imine-linked COF films have been developed, they are less common for 2D COFs with other linkages, such as hydrazone or β-ketoenamine COFs. Hydrazone-linked 2D COFs are chemically stable,[33] highly crystalline[34] materials reinforced with interlayer and intralayer hydrogen bonding[35,36] that originate from the N-H groups in their linkages. Previous reports have shown that hydrogen bonding in 2D COFs can have a positive effect on their surface area, bulk crystallinity,[37] thermal stability,[11] resistance to hydrolysis,[31,38] and mechanical strength.[9,20,39] Due to these factors, hydrazone-linked COFs and β-ketoenamine linked COFs that generate from tautamarization of hydrazone linkages[40] are excellent candidates for lightweight and strong materials that can be tuned for various types of applications. However, only a few examples of COF processing techniques have been reported for 2D-COFs with β-ketoenamine[41] or hydrazone linkages[21,25,42,43] and it remains a challenge to make them *via* solution processing methods such as spin, or drop casting.

Our initial efforts to study solution processable hydrazone COFs used a previously reported method where COFs can be dissolved and reprocessed by drop casting in trifluoroacetic acid (TFA)/water mixtures. This method was reported by Dichtel and co-workers for an imine-linked COF (BND-TFB COF),[17] and used to produce a variety of other imine,[44] and amide-linked films.[39] While successful in these situations, we were unable to dissolve common hydrazone-linked COFs, such as COF-42 (Figure 2A), using this method. We hypothesized that COF-42 was poorly soluble in TFA due to stronger

interlayer hydrogen bonding interactions and greater resistance to protonation owing to the lower pK_a of the hydrazone linkage compared with imine groups.[45,46] To address this issue, we have taken a pore engineering approach which involves adding polyether side chains to the hydrazide monomers to improve the solubility of the delaminated sheets formed after being protonated in an acidic solution. Figure 2 shows the structures and synthetic conditions of the COFs used for this system. COF-PEO-3 (Figure 2B) is a previously reported COF[47] with hydrazone linkages to a triformylbenzene (TFB) node, and TFP-PEO-3 (Figure 2C) is a novel COF that contains highly stable and extremely hydrolytic resistant β-ketoenamine linkages to a triformylphloroglucinol (TFP) node.[31] We synthesized these COFs using conventional solvothermal methods to produce powdered polymeric materials, followed by dissolving them in a trifluoroacetic acid (TFA) and water mixture, which allowed us to use drop casting as a technique to make films.

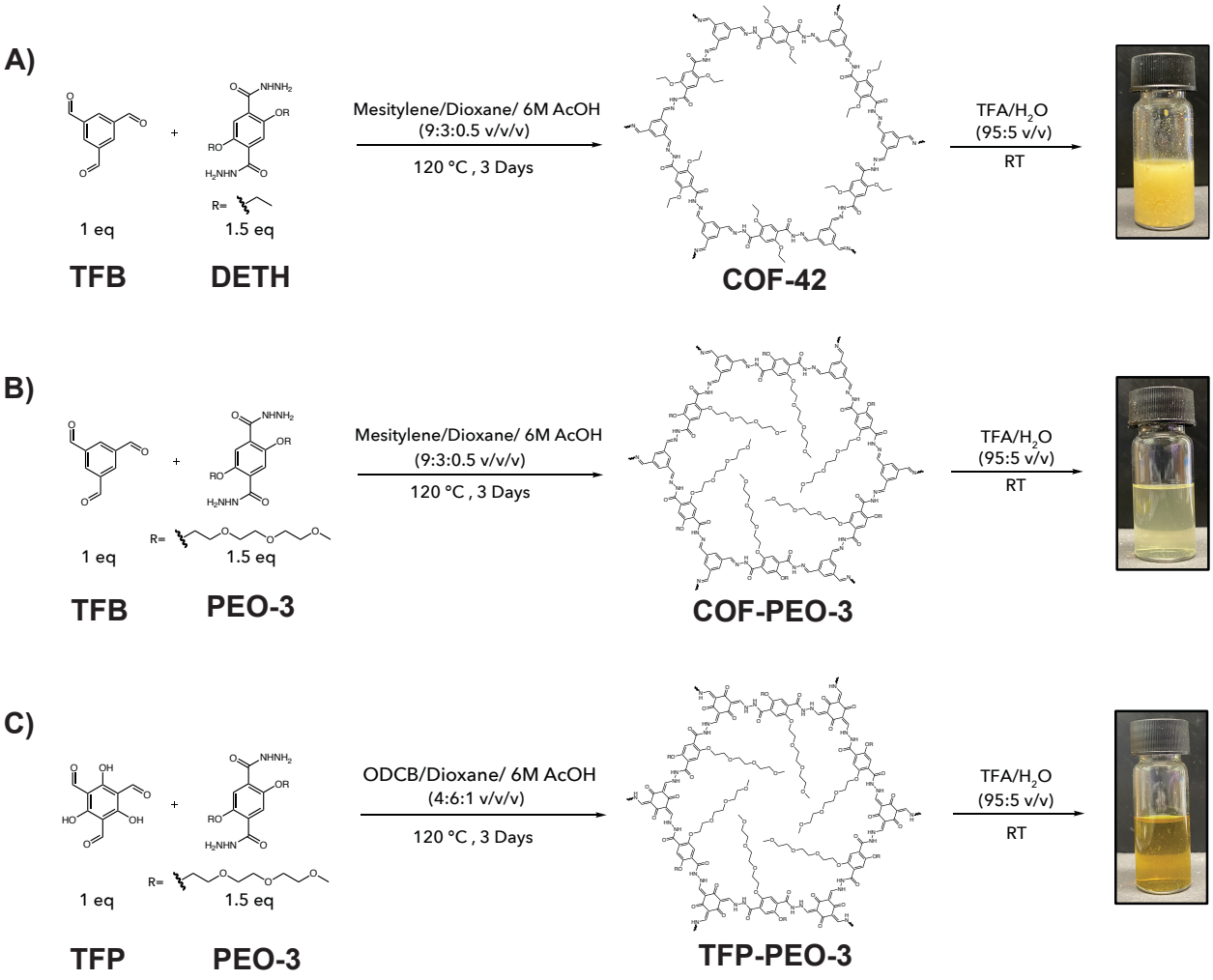

Figure 2. Synthesis conditions and demonstration of COF solubility in TFA/H_2O for (A) COF-42, (B) COF-PEO-3, and (C) TFP-PEO-3 (10 mg/mL solutions).

As these COF films are continuous and free-standing with excellent mechanical flexibility, they provide a solid foundation for flexible dielectric film capacitor applications. To demonstrate this, we employed drop cast films of COF-PEO-3 and TFP-PEO-3 to prepare dielectric devices. Remarkably, the resulting COF films exhibit large dielectric constants (9.6–11.4 at 1 kHz) and high breakdown strengths of >500 MV m^{-1}, which led to high discharged energy densities of 6.87 and 11.22 J cm^{-3} for COF-PEO-3 and TFP-PEO-3, respectively.

Results and Discussion

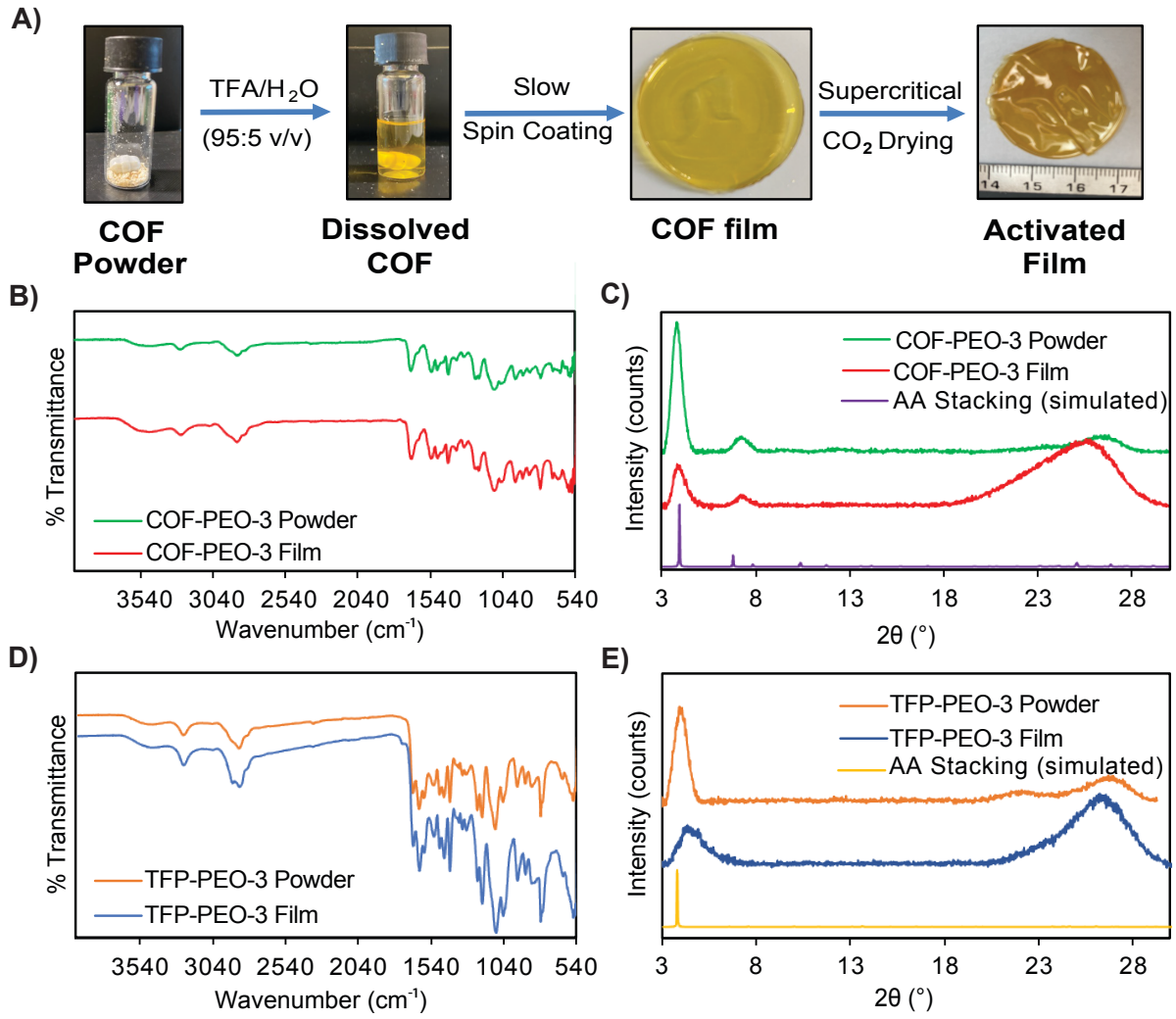

Figure 3. COF film formation and characterization. (A) Workflow for the top-down COF film fabrication of COF-PEO-3. Comparison of (B) IR spectra and (C) PXRD profiles of COF-PEO-3 powder and film. Comparison of (D) IR spectra and (E) PXRD profiles of TFP-PEO-3 powder and film.

FTIR analysis of COF-PEO-3 (Figure S4) and TFP-PEO-3 (Figure S5) show the disappearance of functional groups unique to the starting materials (*e.g.*, aldehyde groups) and the formation of C=N hydrazone linkages, confirming the polymerization for both COFs. A comparison of the FTIR spectra for both COF-PEO-3 powder, and the solution cast film is shown in Figure 3B. The FTIR spectra of the film and powder COF samples are consistent with one another, which indicates that the hydrazone linkages are

preserved during the solution casting process. A similar consistency between the FTIR spectra of the powder and film samples of TFP-PEO-3 was also observed (Figure 3D).

The PXRD pattern (Figure 3C) of COF-PEO-3 agrees with previously reported data.[47] The characteristic peaks for COF PEO-3 at 2θ 3.6° and 7.2° were observed along with a broad peak from 2θ 18° to 29° in the film, which indicates that the framework structure is present after processing. PXRD analysis (Figure 3E) for TFP-PEO-3 shows [100] reflection at 2θ, 3.85° and the 001 reflection at 25.5°. The simulated diffraction pattern generated in the BIOVIA Materials Studio software package is consistent with the experimental pattern (Figure 3E). Crystal geometry optimization was done, and optimized lattice parameters were a = b = 27.15 Å, c = 3.81 Å, $\alpha = \beta = 90°$, $\gamma = 120°$. In eclipsed (AA) stacking mode, the peak at 2θ, 3.85° corresponds to 100 reflections (Figure S9). In the TFP-PEO-3 film sample, this low angle high intense peak was observed at 2θ, 4.08°. This may be a result of a known phenomenon for COFs through exfoliation called interlayer shifting.[48] AA stacking of the dried COF can be changed through dissolving and re-drying. Here the change in 2θ is small ($\Delta 2\theta = 0.23°$) since the effect on the structure is negligible. The broad peak near 2θ, 27° is also observable in both powder and film, representing [001] reflection. The crystallinity of TFP-PEO-3 also decreased during the film formation. ^{1}H NMR studies of COF-PEO-3 and TFP-PEO-3 were carried out in TFA-*d* solvent system (Figures S10 and S11). COFs dissolved in deuterated TFA show shifted peaks from the original positions of the monomers. This is another indication that the frameworks are not fully dissociated into monomers but in different environments may be in the forms of oligomers and exfoliated sheets.[17]

To estimate the performance and durability of a material it is important to quantify its mechanical properties (ultimate tensile strength, toughness, Young's modulus, *etc.*). These values are challenging to obtain in COF-based materials because it is difficult to form a continuous, free-standing film or dog-bone samples that can be measured using conventional tensile testing. As a result, the mechanical properties of many COFs are measured using relatively small samples with nanoindentation methods[8,19] or other specialized techniques.[44,49] Table S1 has summarized some of the pioneering attempts

towards analyzing the strength of pure COF materials. In these examples, analyses using microscopic characterization methods achieved very high Young's moduli. For example, Fang *et al*[20] reported 46.3 GPa Young's modulus for imine-bonded COF films from nanoindentation measurement. Despite this impressive performance the observed scale is very small, and defects or imperfections formed during the casting of the whole film can directly affect the bulk mechanical performance of the material.[44,50] Indeed, most reports of conventional tensile testing studies involving 2D COFs have been carried out on samples of COF/polymer composites rather than free-standing COF films for these reasons.[9,22]

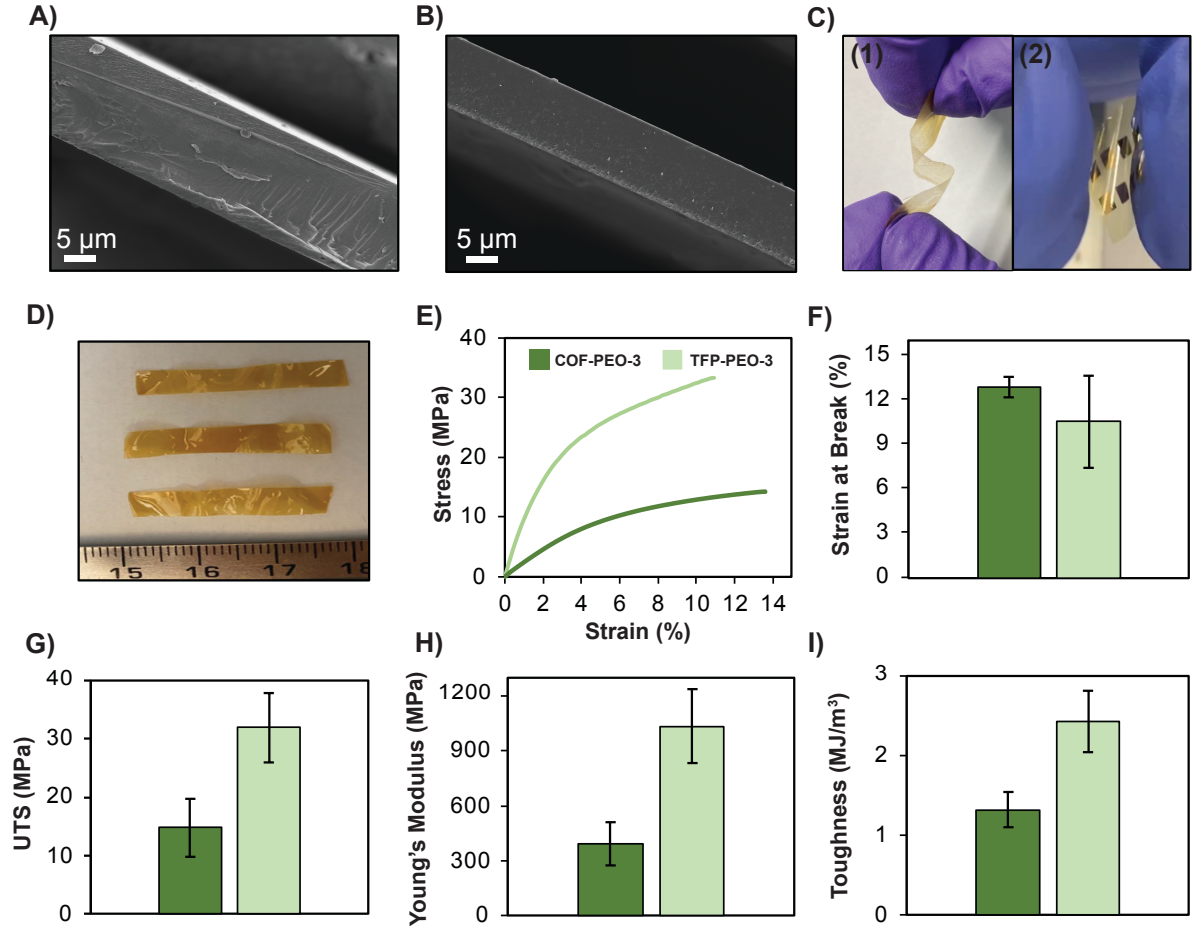

Figure 4. Cross-sectional scanning electron microscopy (SEM) images of (A) COF-PEO-3 and (B) TFP-PEO-3 Top-down films. (C) Demonstration of the flexibility of free-standing COF-PEO-3 films (1) as-prepared and (2) after deposition of electrodes for electrical measurements. (D) Rectangular samples of COF-PEO-3 films prepared for tensile testing. (E) Representative stress-strain curves measured for COF-PEO-3 and TFP-PEO-3. Bar plots showing the (F) strain at break, (G) ultimate tensile strength (UTS), (H) Young's modulus, and (I) toughness values for each of the COF films.

The morphology of the synthesized films was analyzed using scanning electron microscopy (SEM) (Figures 4A, 4B, and S15). Both the COF-PEO-3 and TFP-PEO-3 films have a smooth, dense, and continuous appearance. Moreover, these films are highly flexible and can be easily cut into shapes without cracking (Figures 4C and 4D). Representative stress-strain curves for these samples are shown in Figure 4E. COF-PEO-3 has an ultimate tensile strength of 14.8±2.2 MPa, a strain at break of 12.8±0.7%, Young's modulus of 391.8±118.7 MPa and toughness of 1.3±0.2 MJ m^{-3} (Figures 4F-I). TFP-PEO-3 has an ultimate tensile strength of 32.0±5.9 MPa, strain at break 10.5±3.1%, Young's modulus of 1034.7±201.2 MPa and toughness of 2.4±0.4 MJ m^{-3} (Figures 4F-I). Compared to the COF-PEO-3 films, the TFP-PEO-3 films were stiffer, tougher, and had greater overall strength, as represented by a 164% increase in Young's modulus, an 86% increase in toughness, and a 116% increase in the ultimate tensile strength. A possible explanation for this may be related to the increased amount of hydrogen bonding in TFP-PEO-3 compared to COF-PEO-3. It is well known that polymer networks with extensive hydrogen bonding, such as Kevlar, exhibit exceptional mechanical properties.[51] The TFP node has three additional hydroxyl groups than the TFB monomer. Keto formation of the TFP-PEO-3 in computational models (Figure S12) shows these three extra oxygens in TFP can act as acceptors to hydrogen bonding and that the one extra hydrogen on the hydrazone nitrogen atom acts as a hydrogen bond donor (Figure 5A). Opportunities for interlayer hydrogen bonding[36] are also higher for TFP-PEO-3 than COF-PEO-3 due to the presence of more hydrogen bond donors and acceptors.

The BET surface areas for the COF powders and films were measured by nitrogen gas adsorption at 77 K. The previously reported BET surface area for COF-PEO-3 powder (13 m^2 g^{-1}) is very low[47] and the COF-PEO-3 film did not demonstrate any porosity. The BET surface area (Figure S13) of the TFP-PEO-3 powder is 34 m^2 g^{-1} and the film has a BET surface area of 5 m^2 g^{-1}. The low surface areas observed in all the COF polymers described here are attributed to the polyethylene glycol chains filling and blocking the pore accessibility. Nonetheless, the low BET surface area of these COF films is compensated for not only by their excellent mechanical strength, flexibility, and self-

standing capability, but also by their large dielectric constant and remarkable electrical breakdown strength (see the discussion below). Thermogravimetric (TGA) analysis shows (Figure S14) that both COF films are stable up to 300 °C and both synthesized films show the same thermal behavior as their COF powder counterparts.

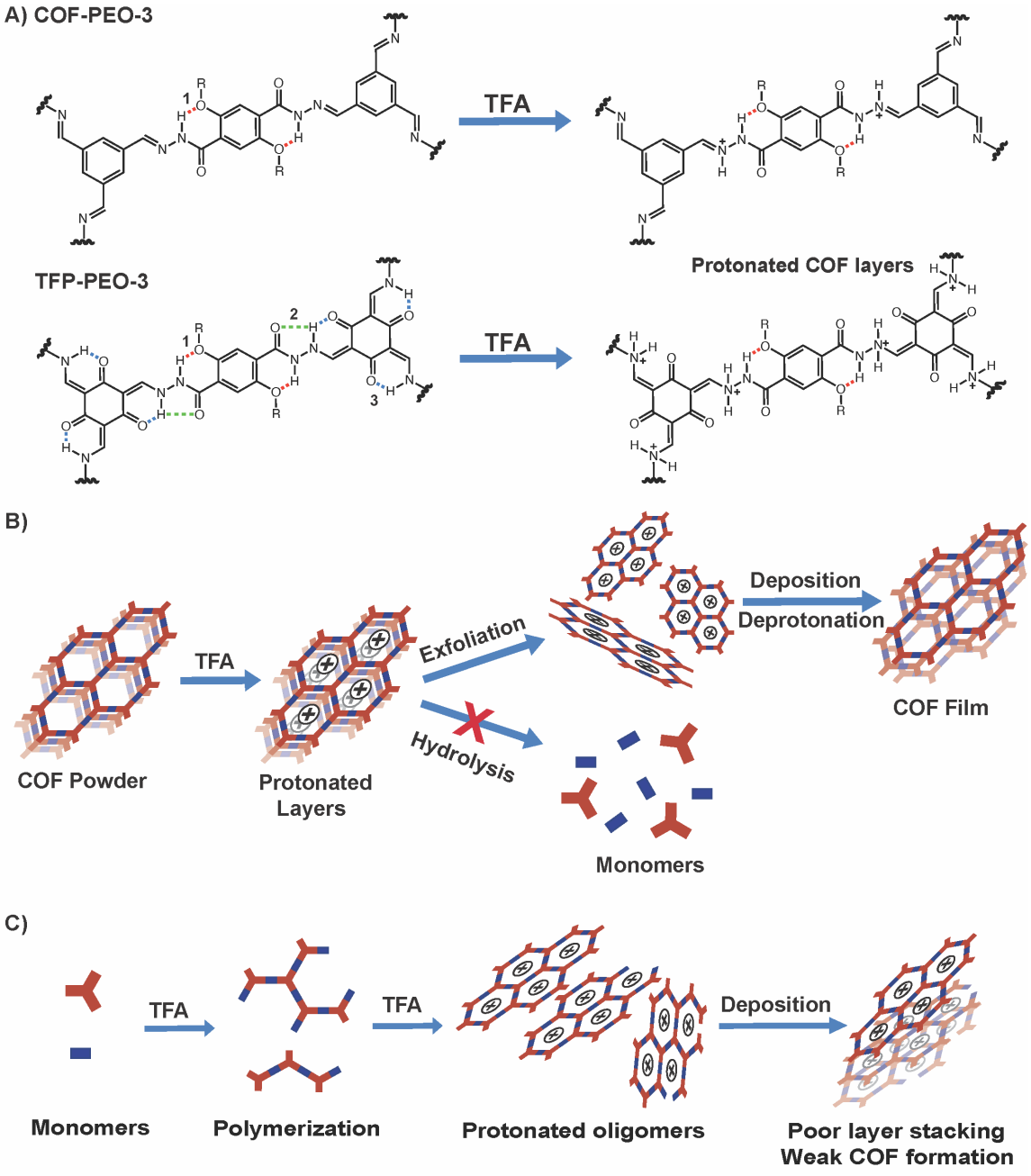

Figure 5. (A) Examples of intralayer hydrogen bonding interactions possible for COF-PEO-3 and TFP-PEO-3 structures. (B) Illustrations of potential mechanistic pathways for solution processing pre-synthesized COF material and (C) monomer precursor solutions, in TFA.

As described in Figure 5, solution processing of COFs in TFA works by protonation of basic sites, such as nitrogen and oxygen atoms, in the polymer structure, which can disrupt the non-covalent interactions that hold the 2D layers together.[17] In hydrazone-linked COFs, the extent of this protonation is not enough to completely solubilize the COF. This may be because, compared to imine-linked COFs which largely rely upon van der Waals or aromatic stacking interactions to maintain their eclipsed structures, hydrazone COFs contain a variety of interlayer hydrogen bonding interactions alongside the van der Waals and π-stacking forces. In addition to potentially stronger interlayer attraction in hydrazone COFs, the pK_a values of protonated hydrazone linkage are lower than[45,46] comparable imine linkages,[52] which may result in a lower concentration of protonated sites in the hydrazone COF, making them more resistant to exfoliation. The addition of the triethylene glycol sidechains can provide additional interactions with the polar TFA solvent that will overcome the reduced protonation, allowing the hydrazone COFs to be exfoliated in solution. Compared to COF-PEO-3, TFP-PEO-3 takes longer to dissolve with stirring, indicating a higher resistance to exfoliation potentially due to the higher density of hydrogen bonding present in the structure (Figure 5A). It is possible that after exfoliation, the highly acidic environment could cause hydrolysis of the reversible COF linkages to regenerate the monomers (Figure 5B). However, we have not observed this by FT-IR or PXRD. Therefore, we hypothesize that exfoliation is the major pathway in the dissolution process for both COFs.

To test an alternative method for hydrazone COF film formation, we carried out a “bottom-up” synthesis approach where the monomers for each COF are directly dissolved in TFA and cast into films and then subjected to conventional solvothermal conditions in film form (Figure S6). This approach has previously been shown to be effective with some imine-linked COFs.[29] FT-IR spectra of these prepared films (Figure S7) match those of the respective original COF powders, indicating that the hydrazone or β-ketoenamine bonds have formed. PXRDs of these films also show some of the characteristic peaks for the corresponding COFs (Figure S8), but the amorphous nature has increased as indicated by the large, broad peaks at higher angles. When these films were subjected to mechanical testing, mechanical properties are universally poorer when compared with

films synthesized from dissolving the COF powders (*i.e.,* the "top-down" approach). The large error values in our mechanical test measurements of films synthesized from monomers compared to those made from pre-synthesized COFs indicates that the "bottom-up" approach produces materials with inconsistent fractions of 2D COF polymer (*vs.* amorphous material) or a larger number of defects that result in premature mechanical failure. The shape of the stress-strain curves of these bottom-up approach films are different than that of top-down approach films (Figures S16 and 4E). For the films from bottom-up synthesis, most of the stress-strain curves reach a yield plateau region[53] where the gradient is nearly zero. COF-PEO-3 (bottom-up) has an ultimate tensile strength of 7.4±3.0 MPa, strain at break 4.9±1.8 %, Young's modulus of 265.4±117.0 MPa and toughness of 0.3±0.1 MJ m^{-3} (Figures S17), whereas TFP-PEO-3 (bottom-up) has an ultimate tensile strength of 17.4±7.4 MPa, strain at break 12.3±7.5 %, Young's modulus of 301.8±86.0 MPa and toughness of 1.0±0.5 MJ m^{-3} (Figures S17). For COF-PEO-3 films synthesized from monomers, the Young's modulus has decreased by 32%, the strain at break has decreased by 62% and the toughness has decreased by 77% compared to the top-down synthesis of the same COF film. For the TFP-PEO-3 film obtained the bottom-up method similarly reduced properties were observed. The Young's modulus decreased by 71%, the ultimate tensile strength decreased by 45%, and the toughness decreased by 58% compared to the top-down synthesis of the same COF film. We hypothesize that the mechanically weak films formed from the bottom-up synthesis are a result of poor COF sheet formation in the presence of the highly acidic TFA solution (Figure 5C). When the monomers are dissolved in TFA, the resulting polymer is already protonated thereby reducing the interlayer stacking interactions and disrupting the formation of an extended crystalline network.

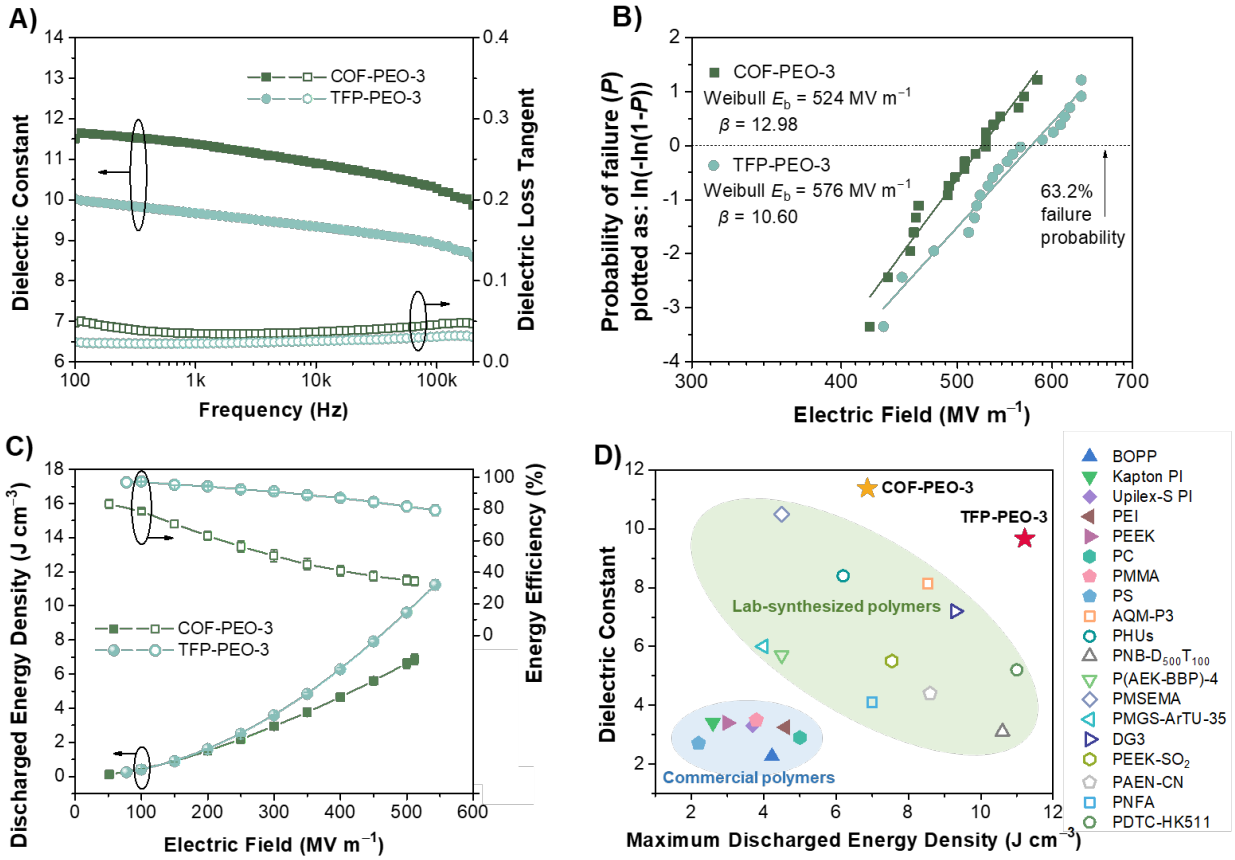

Figure 6. Dielectric and energy storage properties of COF films. (A) Frequency-dependent dielectric spectra of COF films. (B) Weibull statistics of dielectric breakdown strength of COF films. (C) Discharged energy density and energy efficiency as a function of electric field of COF films. (D) Correlation between the maximum discharged energy density and dielectric constant (at 1 kHz) among COF-PEO-3, TFP-PEO-3 and other dielectrically linear commercial polymers as well as most recent noteworthy lab-synthesized polymers. BOPP: biaxially oriented polypropylene; PI: polyimide; PEI: polyetherimide; PEEK: polyether ether ketone; PC: polycarbonate; PMMA: poly(methyl methacrylate); PS: polystyrene. The representative values were obtained from the literature and are detailed in Table S2.

To demonstrate the utility of our solution processing method, we fabricated several dielectric devices using COF-PEO-3 and TFP-PEO-3 films. The films produced using the "top-down" processing method feature excellent flexibility and mechanical strength – properties that are essential in dielectric film capacitor applications.[54,55,56] Thanks to the relatively polar molecular structures, low BET surface areas as well as the continuous and defect-free film structures (as evidenced by cross-sectional SEM images in Figures 4A, 4B and S15), both COF films display high dielectric constant as seen in Figure 6A.

Specifically, at 1 kHz, the dielectric constant of COF-PEO-3 and TFP-PEO-3 films are as high as 11.38 and 9.67, respectively, among the highest for dielectrically linear polymers[57,58] and comparable to, or even higher than, ferroelectric polymers such as PVDF-based homopolymers and copolymers.[59,60] Furthermore, both films exhibit low dielectric loss tangents (<0.05) across the investigated frequency range.

Statistical analysis indicates that both COF films have dielectric breakdown strengths greater than 500 MV m^{-1}, as plotted in Figure 6B, making them suitable for high-voltage applications. When integrated in dielectric capacitor devices, TFP-PEO-3 shows superior dielectric energy storage performance than COF-PEO-3 (Figure 6C). In particular, TFP-PEO-3 demonstrates excellent energy storage performance, with a maximum energy density of 11.22 J cm^{-3} and an efficiency of ~80% at 543 MV m^{-1}, while COF-PEO-3 achieves a maximum energy density of 6.87 J cm^{-3} and an efficiency of <40% at 512 MV m^{-1}. Leakage current (Figure S18) and thermally stimulated depolarization current (TSDC, Figure S19) tests further reveal that TFP-PEO-3 exhibits smaller electricity leakage and more trapped charges,[61,62] corroborating with its better electrical insulating capacity (i.e., higher breakdown strength and energy efficiency) than COF-PEO-3. The discharged energy density of TFP-PEO-3 exceeds that of commercial dielectric polymers such as biaxially oriented polypropylene (BOPP) and polyvinylidene difluoride (PVDF) films (Figure S20), and most recent noteworthy literature results of lab-synthesized dielectrically linear polymers, as summarized in Table S2 and shown in Figure 6D, suggesting its great potential for flexible energy storage device applications under high electric fields.

Conclusions

We have developed a pore engineering strategy for designing solution processable hydrazone-linked COFs. This approach allows for the straightforward solution casting of COFs with hydrolytically resistant dynamic linkages, and strong non-covalent interlayer interactions. In this study, 2D-COFs with solubilizing sidechains in their pores (COF-PEO-

3 and TFP-PEO-3) can be dissolved into a homogeneous solution in TFA, and drop cast into continuous, free-standing films. Mechanical testing was carried out for COF films prepared with different structural compositions and using different methods of film preparation. We found that these factors had significant effects not only on the mechanical parameters, but also on the reproducibility of the film casting process, with films being produced from solution cast COF powders being universally more consistent, and with better mechanical strength. It was further revealed that TFP-PEO-3 was stiffer and stronger than COF-PEO-3, which we attribute to the increased amount of functional group sites available to form hydrogen bonding interactions. The large difference in mechanical quality between the COF films produced from monomers or pre-synthesized COF offers additional mechanistic insight into the process of COF dissolution and precipitation. The TFP-PEO-3 films obtained using a "top-down" synthesis approach display remarkable mechanical strength and electrical insulating properties, characterized by a large dielectric constant, high breakdown strength, and superior energy density when embodied in flexible film capacitor devices.

ASSOCIATED CONTENT

Supporting Information

^{1}H NMR, FT-IR, TGA, SEM, leakage current, TSDC, digital photographs, dielectric performance comparisons and computational models are included in the Supporting Information.

AUTHOR INFORMATION

† These authors contributed equally

Corresponding Authors

*Ronald A. Smaldone – Department of Chemistry and Biochemistry, University of Texas at Dallas, Richardson, Texas 75080, United States; Email: ronald.smaldone@utdallas.edu

*Yi Liu – Lawrence Berkeley National Laboratory, The Molecular Foundry and Materials Sciences Division, Lawrence Berkeley National Laboratory, Berkeley, California, 94720, United States. Email: yliu@lbl.gov

Authors

Milinda C. Senarathna – Department of Chemistry and Biochemistry, University of Texas at Dallas, Richardson, Texas 75080, United States; https://orcid.org/0000-0002-9359-317X.

He Li – Lawrence Berkeley National Laboratory, The Molecular Foundry and Materials Sciences Division, Lawrence Berkeley National Laboratory, Berkeley, California, 94720, United States. https://orcid.org/0000-0002-4076-7279.

Sachini D. Perera – Department of Chemistry and Biochemistry, University of Texas at Dallas, Richardson, Texas 75080, United States.

Jose Torres-Correas – Department of Chemistry and Biochemistry, University of Texas at Dallas, Richardson, Texas 75080, United States.

Shashini D. Diwakara – Department of Chemistry and Biochemistry, University of Texas at Dallas, Richardson, Texas 75080, United States.

Samuel R. Boardman – Department of Chemistry and Biochemistry, University of Texas at Dallas, Richardson, Texas 75080, United States.

Author Contribution

R.A.S and Y.L.conceived the project and secured funding. M.C.S designed, synthesized, and characterized the COFs. H.L fabricated electrical devices, conducted electrical measurements and SEM characterization. S.D.P assisted with tensile testing and analysis of the mechanical characterization data. J.T, S.D.D, S.R.B assisted with monomer synthesis and characterization. All authors contributed to the reviewing and editing the manuscript.

ACKNOWLEDGMENT

R.A.S. acknowledges support from UT Dallas and the Army Research Laboratory (W911NF-18-2-0035) and the American Chemical Society Petroleum Research Fund

(PRF#61360- ND10). H.L. and Y.L. were funded by the U.S. Department of Energy, Office of Science, Office of Basic Energy Sciences, Materials Sciences and Engineering Division under Contract No. DE-AC02-05CH11231 within the Inorganic/Organic Nanocomposites Program (KC3104). Part of the work was carried out at the Molecular Foundry, a user facility supported by the Office of Science, Office of Basic Energy Sciences, of the U.S. Department of Energy under Contract No. DE-AC02-05CH11231. The authors thank Dr. Steve W. Shelton and Liana M. Klivansky at the Molecular Foundry for instrumental support.

References

1. Côté, A.P., Benin, A.I., Ockwig, N.W., O'Keeffe, M., Matzger, A.J., and Yaghi, O.M. (2005). Porous, Crystalline, Covalent Organic Frameworks. Science *310*, 1166–1170. 10.1126/science.1120411.

2. Zhan, X., Chen, Z., and Zhang, Q. (2017). Recent progress in two-dimensional COFs for energy-related applications. J. Mater. Chem. A *5*, 14463–14479. 10.1039/C7TA02105D.

3. Dey, K., Pal, M., Rout, K.C., Kunjattu H, S., Das, A., Mukherjee, R., Kharul, U.K., and Banerjee, R. (2017). Selective Molecular Separation by Interfacially Crystallized Covalent Organic Framework Thin Films. J. Am. Chem. Soc. *139*, 13083–13091. 10.1021/jacs.7b06640.

4. Kandambeth, S., Biswal, B.P., Chaudhari, H.D., Rout, K.C., Kunjattu H., S., Mitra, S., Karak, S., Das, A., Mukherjee, R., Kharul, U.K., et al. (2017). Selective Molecular Sieving in Self-Standing Porous Covalent-Organic-Framework Membranes. Adv. Mater. *29*, 1603945. 10.1002/adma.201603945.

5. Guo, J., and Jiang, D. (2020). Covalent Organic Frameworks for Heterogeneous Catalysis: Principle, Current Status, and Challenges. ACS Cent. Sci. *6*, 869–879. 10.1021/acscentsci.0c00463.

6. Shao, P., Li, J., Chen, F., Ma, L., Li, Q., Zhang, M., Zhou, J., Yin, A., Feng, X., and Wang, B. (2018). Flexible Films of Covalent Organic Frameworks with Ultralow Dielectric Constants under High Humidity. Angew. Chem. Int. Ed. *57*, 16501–16505. 10.1002/anie.201811250.

7. Evans, A.M., Giri, A., Sangwan, V.K., Xun, S., Bartnof, M., Torres-Castanedo, C.G., Balch, H.B., Rahn, M.S., Bradshaw, N.P., Vitaku, E., et al. (2021). Thermally

conductive ultra-low-k dielectric layers based on two-dimensional covalent organic frameworks. Nat. Mater. *20*, 1142–1148. 10.1038/s41563-021-00934-3.

8. Fang, Q., Sui, C., Wang, C., Zhai, T., Zhang, J., Liang, J., Guo, H., Sandoz-Rosado, E., and Lou, J. (2021). Strong and flaw-insensitive two-dimensional covalent organic frameworks. Matter *4*, 1017–1028. 10.1016/j.matt.2021.01.001.

9. Sandoz-Rosado, E., Beaudet, T.D., Andzelm, J.W., and Wetzel, E.D. (2018). High strength films from oriented, hydrogen-bonded "graphamid" 2D polymer molecular ensembles. Sci. Rep. *8*, 3708. 10.1038/s41598-018-22011-7.

10. Croy, A., Raptakis, A., Bodesheim, D., Dianat, A., and Cuniberti, G. (2022). Toward Coarse-Grained Elasticity of Single-Layer Covalent Organic Frameworks. J. Phys. Chem. C *126*, 18943–18951. 10.1021/acs.jpcc.2c06268.

11. Lustig, S.R., Andzelm, J.W., and Wetzel, E.D. (2021). Highly Thermostable Dynamic Structures of Polyaramid Two-Dimensional Polymers. Macromolecules *54*, 1291–1303. 10.1021/acs.macromol.0c01931.

12. Hao, W., Zhao, Y., Miao, L., Cheng, G., Zhao, G., Li, J., Sang, Y., Li, J., Zhao, C., He, X., et al. (2023). Multiple Impact-Resistant 2D Covalent Organic Framework. Nano Lett., acs.nanolett.2c04747. 10.1021/acs.nanolett.2c04747.

13. Lee, C., Wei, X., Kysar, J.W., and Hone, W. (2008). Measurement of the Elastic Properties and Intrinsic Strength of Monolayer Graphene. Science *321*, 385–388. 10.1126/science.1156211.

14. Desyatkin, V.G., Martin, W.B., Aliev, A.E., Chapman, N.E., Fonseca, A.F., Galvão, D.S., Miller, E.R., Stone, K.H., Wang, Z., Zakhidov, D., et al. (2022). Scalable Synthesis and Characterization of Multilayer γ-Graphyne, New Carbon Crystals with a Small Direct Band Gap. J. Am. Chem. Soc. *144*, 17999–18008. 10.1021/jacs.2c06583.

15. Lu, J., Lin, F., Wen, Q., Qi, Q.-Y., Xu, J.-Q., and Zhao, X. (2019). Large-scale synthesis of azine-linked covalent organic frameworks in water and promoted by water. New J. Chem. *43*, 6116–6120. 10.1039/C9NJ00830F.

16. Li, X., Qiao, J., Chee, S.W., Xu, H.-S., Zhao, X., Choi, H.S., Yu, W., Quek, S.Y., Mirsaidov, U., and Loh, K.P. (2020). Rapid, Scalable Construction of Highly Crystalline Acylhydrazone Two-Dimensional Covalent Organic Frameworks via Dipole-Induced Antiparallel Stacking. J. Am. Chem. Soc. *142*, 4932–4943. 10.1021/jacs.0c00553.

17. Burke, D.W., Sun, C., Castano, I., Flanders, N.C., Evans, A.M., Vitaku, E., McLeod, D.C., Lambeth, R.H., Chen, L.X., Gianneschi, N.C., et al. (2020). Acid Exfoliation of Imine-linked Covalent Organic Frameworks Enables Solution Processing into Crystalline Thin Films. Angew. Chem. Int. Ed. *59*, 5165–5171. 10.1002/anie.201913975.

18. Wang, S., Wang, Q., Shao, P., Han, Y., Gao, X., Ma, L., Yuan, S., Ma, X., Zhou, J., Feng, X., et al. (2017). Exfoliation of Covalent Organic Frameworks into Few-Layer Redox-Active Nanosheets as Cathode Materials for Lithium-Ion Batteries. J. Am. Chem. Soc. *139*, 4258–4261. 10.1021/jacs.7b02648.

19. Dey, K., Bhunia, S., Sasmal, H.S., Reddy, C.M., and Banerjee, R. (2021). Self-Assembly-Driven Nanomechanics in Porous Covalent Organic Framework Thin Films. J. Am. Chem. Soc. *143*, 955–963. 10.1021/jacs.0c11122.

20. Fang, Q., Pang, Z., Ai, Q., Liu, Y., Zhai, T., Steinbach, D., Gao, G., Zhu, Y., Li, T., and Lou, J. (2023). Superior mechanical properties of multilayer covalent-organic frameworks enabled by rationally tuning molecular interlayer interactions. Proc. Natl. Acad. Sci. *120*, e2208676120. 10.1073/pnas.2208676120.

21. Wang, Z., Yu, Q., Huang, Y., An, H., Zhao, Y., Feng, Y., Li, X., Shi, X., Liang, J., Pan, F., et al. (2019). PolyCOFs: A New Class of Freestanding Responsive Covalent Organic Framework Membranes with High Mechanical Performance. ACS Cent. Sci. *5*, 1352–1359. 10.1021/acscentsci.9b00212.

22. Xu, J., He, Y., Bi, S., Wang, M., Yang, P., Wu, D., Wang, J., and Zhang, F. (2019). An Olefin-Linked Covalent Organic Framework as a Flexible Thin-Film Electrode for a High-Performance Micro-Supercapacitor. Angew. Chem. Int. Ed. *58*, 12065–12069. 10.1002/anie.201905713.

23. Roesner, E.K., Asheghali, D., Kirillova, A., Strauss, M.J., Evans, A.M., Becker, M.L., and Dichtel, W.R. (2022). Arene–perfluoroarene interactions confer enhanced mechanical properties to synthetic nanotubes. Chem. Sci., 10.1039.D1SC05932G. 10.1039/D1SC05932G.

24. Liang, R.-R., A, R.-H., Xu, S.-Q., Qi, Q.-Y., and Zhao, X. (2020). Fabricating Organic Nanotubes through Selective Disassembly of Two-Dimensional Covalent Organic Frameworks. J. Am. Chem. Soc. *142*, 70–74. 10.1021/jacs.9b11401.

25. Liu, Z., Zhang, K., Huang, G., Xu, B., Hong, Y., Wu, X., Nishiyama, Y., Horike, S., Zhang, G., and Kitagawa, S. (2022). Highly Processable Covalent Organic Framework Gel Electrolyte Enabled by Side-Chain Engineering for Lithium-Ion Batteries. Angew. Chem. Int. Ed. *61*. 10.1002/anie.202110695.

26. Carrington, M.E., Rampal, N., Madden, D.G., O'Nolan, D., Casati, N.P.M., Divitini, G., Martín-Illán, J.Á., Tricarico, M., Cepitis, R., Çamur, C., et al. (2022). Sol-gel processing of a covalent organic framework for the generation of hierarchically porous monolithic adsorbents. Chem *8*, 2961–2977. 10.1016/j.chempr.2022.07.013.

27. Missale, E., Frasconi, M., and Pantano, M.F. (2023). Ultrathin organic membranes: Can they sustain the quest for mechanically robust device applications? iScience *26*, 105924. 10.1016/j.isci.2023.105924.

28. Matsumoto, M., Valentino, L., Stiehl, G.M., Balch, H.B., Corcos, A.R., Wang, F., Ralph, D.C., Mariñas, B.J., and Dichtel, W.R. (2018). Lewis-Acid-Catalyzed Interfacial Polymerization of Covalent Organic Framework Films. Chem *4*, 308–317. 10.1016/j.chempr.2017.12.011.

29. Barnes, M.G., McLeod, D.C., and Lambeth, R.H. (2022). Highly Crystalline, Free-Standing Covalent Organic Framework Films Produced Directly from Monomer Solutions. ACS Appl. Polym. Mater. *4*, 2017–2021. 10.1021/acsapm.1c01828.

30. Berlanga, I., Mas-Ballesté, R., and Zamora, F. (2012). Tuning delamination of layered covalent organic frameworks through structural design. Chem. Commun. *48*, 7976. 10.1039/c2cc32187d.

31. Chandra, S., Kandambeth, S., Biswal, B.P., Lukose, B., Kunjir, S.M., Chaudhary, M., Babarao, R., Heine, T., and Banerjee, R. (2013). Chemically Stable Multilayered Covalent Organic Nanosheets from Covalent Organic Frameworks via Mechanical Delamination. J. Am. Chem. Soc. *135*, 17853–17861. 10.1021/ja408121p.

32. Martín-Illán, J.Á., Suárez, J.A., Gómez-Herrero, J., Ares, P., Gallego-Fuente, D., Cheng, Y., Zhao, D., Maspoch, D., and Zamora, F. (2022). Ultralarge Free-Standing Imine-Based Covalent Organic Framework Membranes Fabricated via Compression. Adv. Sci. *9*, 2104643. 10.1002/advs.202104643.

33. Li, X., Cai, S., Sun, B., Yang, C., Zhang, J., and Liu, Y. (2020). Chemically Robust Covalent Organic Frameworks: Progress and Perspective. Matter *3*, 1507–1540. 10.1016/j.matt.2020.09.007.

34. Uribe-Romo, F.J., Doonan, C.J., Furukawa, H., Oisaki, K., and Yaghi, O.M. (2011). Crystalline Covalent Organic Frameworks with Hydrazone Linkages. J. Am. Chem. Soc. *133*, 11478–11481. 10.1021/ja204728y.

35. Diwakara, S.D., McCandless, G.T., Alahakoon, S.B., and Smaldone, R.A. (2021). Synthesis of Side-Chain-Free Hydrazone-Linked Covalent Organic Frameworks through Supercritical Carbon Dioxide Activation. Org. Mater. *03*, 277–282. 10.1055/a-1477-5123.

36. Li, X., Gao, Q., Wang, J., Chen, Y., Chen, Z.-H., Xu, H.-S., Tang, W., Leng, K., Ning, G.-H., Wu, J., et al. (2018). Tuneable near white-emissive two-dimensional covalent organic frameworks. Nat. Commun. *9*, 2335. 10.1038/s41467-018-04769-6.

37. Alahakoon, S.B., Tan, K., Pandey, H., Diwakara, S.D., McCandless, G.T., Grinffiel, D.I., Durand-Silva, A., Thonhauser, T., and Smaldone, R.A. (2020). 2D-Covalent Organic Frameworks with Interlayer Hydrogen Bonding Oriented through Designed Nonplanarity. J. Am. Chem. Soc. *142*, 12987–12994. 10.1021/jacs.0c03409.

38. Halder, A., Ghosh, M., Khayum M, A., Bera, S., Addicoat, M., Sasmal, H.S., Karak, S., Kurungot, S., and Banerjee, R. (2018). Interlayer Hydrogen-Bonded Covalent

Organic Frameworks as High-Performance Supercapacitors. J. Am. Chem. Soc. *140*, 10941–10945. 10.1021/jacs.8b06460.

39. Zeng, Y., Gordiichuk, P., Ichihara, T., Zhang, G., Sandoz-Rosado, E., Wetzel, E.D., Tresback, J., Yang, J., Kozawa, D., Yang, Z., et al. (2022). Irreversible synthesis of an ultrastrong two-dimensional polymeric material. Nature *602*, 91–95. 10.1038/s41586-021-04296-3.

40. Yu, J., Lan, J., Wang, S., Zhang, P., Liu, K., Yuan, L., Chai, Z., and Shi, W. (2021). Robust covalent organic frameworks with tailor-made chelating sites for synergistic capture of U(VI) ions from highly acidic radioactive waste. Dalton Trans. *50*, 3792–3796. 10.1039/D1DT00186H.

41. Kang, Z., Peng, Y., Qian, Y., Yuan, D., Addicoat, M.A., Heine, T., Hu, Z., Tee, L., Guo, Z., and Zhao, D. (2016). Mixed Matrix Membranes (MMMs) Comprising Exfoliated 2D Covalent Organic Frameworks (COFs) for Efficient CO_2 Separation. Chem. Mater. *28*, 1277–1285. 10.1021/acs.chemmater.5b02902.

42. Bunck, D.N., and Dichtel, W.R. (2013). Bulk Synthesis of Exfoliated Two-Dimensional Polymers Using Hydrazone-Linked Covalent Organic Frameworks. J. Am. Chem. Soc. *135*, 14952–14955. 10.1021/ja408243n.

43. Mao, T., Liu, Z., Guo, X., Wang, Z., Liu, J., Wang, T., Geng, S., Chen, Y., Cheng, P., and Zhang, Z. (2023). Engineering Covalent Organic Frameworks with Polyethylene Glycol as Self-Sustained Humidity-Responsive Actuators. Angew. Chem. Int. Ed. *62*. 10.1002/anie.202216318.

44. Zhu, D., Hu, Z., Rogers, T.K., Barnes, M., Tseng, C.-P., Mei, H., Sassi, L.M., Zhang, Z., Rahman, M.M., Ajayan, P.M., et al. (2021). Patterning, Transfer, and Tensile Testing of Covalent Organic Framework Films with Nanoscale Thickness. Chem. Mater. *33*, 6724–6730. 10.1021/acs.chemmater.1c01179.

45. Harnsberger, H.F., Cochran, E.L., and Szmant, H.H. (1955). The Basicity of Hydrazones. J. Am. Chem. Soc. *77*, 5048–5050. 10.1021/ja01624a032.

46. Kalia, J., and Raines, R.T. (2008). Hydrolytic Stability of Hydrazones and Oximes. Angew. Chem. Int. Ed. *47*, 7523–7526. 10.1002/anie.200802651.

47. Zhang, G., Hong, Y., Nishiyama, Y., Bai, S., Kitagawa, S., and Horike, S. (2019). Accumulation of Glassy Poly(ethylene oxide) Anchored in a Covalent Organic Framework as a Solid-State Li^+ Electrolyte. J. Am. Chem. Soc. *141*, 1227–1234. 10.1021/jacs.8b07670.

48. Kang, C., Zhang, Z., Wee, V., Usadi, A.K., Calabro, D.C., Baugh, L.S., Wang, S., Wang, Y., and Zhao, D. (2020). Interlayer Shifting in Two-Dimensional Covalent Organic Frameworks. J. Am. Chem. Soc. *142*, 12995–13002. 10.1021/jacs.0c03691.

49. Khalil, S., Meyer, M.D., Alazmi, A., Samani, M.H.K., Huang, P.-C., Barnes, M., Marciel, A.B., and Verduzco, R. (2022). Enabling Solution Processable COFs through Suppression of Precipitation during Solvothermal Synthesis. ACS Nano, acsnano.2c08580. 10.1021/acsnano.2c08580.

50. Li, H., and Brédas, J.-L. (2021). Impact of Structural Defects on the Elastic Properties of Two-Dimensional Covalent Organic Frameworks (2D COFs) under Tensile Stress. Chem. Mater. *33*, 4529–4540. 10.1021/acs.chemmater.1c00895.

51. Cheng, M., Chen, W., and Weerasooriya, T. (2005). Mechanical Properties of Kevlar® KM2 Single Fiber. J. Eng. Mater. Technol. *127*, 197–203. 10.1115/1.1857937.

52. Buist, G.J., and Lucas, H.J. (1957). Basicity Constants and Rates of Hydration of Some Imines [1]. J. Am. Chem. Soc. *79*, 6157–6160. 10.1021/ja01580a014.

53. Sadowski, A.J., Michael Rotter, J., Stafford, P.J., Reinke, T., and Ummenhofer, T. (2017). On the gradient of the yield plateau in structural carbon steels. J. Constr. Steel Res. *130*, 120–130. 10.1016/j.jcsr.2016.11.024.

54. Wu, C., Deshmukh, A.A., Chen, L., Ramprasad, R., Sotzing, G.A., and Cao, Y. (2022). Rational design of all-organic flexible high-temperature polymer dielectrics. Matter *5*, 2615–2623. 10.1016/j.matt.2022.06.064.

55. Li, H., Zhou, Y., Liu, Y., Li, L., Liu, Y., and Wang, Q. (2021). Dielectric polymers for high-temperature capacitive energy storage. Chem. Soc. Rev. *50*, 6369–6400. 10.1039/D0CS00765J.

56. Li, H., Chang, B.S., Kim, H., Xie, Z., Lainé, A., Ma, L., Xu, T., Yang, C., Kwon, J., Shelton, S.W., et al. (2023). High-performing polysulfate dielectrics for electrostatic energy storage under harsh conditions. Joule *7*, 95–111. 10.1016/j.joule.2022.12.010.

57. Wei, J., and Zhu, L. (2020). Intrinsic polymer dielectrics for high energy density and low loss electric energy storage. Prog. Polym. Sci. *106*, 101254. 10.1016/j.progpolymsci.2020.101254.

58. Le Goupil, F., Salvado, V., Rothan, V., Vidil, T., Fleury, G., Cramail, H., and Grau, E. (2023). Bio-Based Poly(hydroxy urethane)s for Efficient Organic High-Power Energy Storage. J. Am. Chem. Soc. *145*, 4583–4588. 10.1021/jacs.2c12090.

59. Feng, Q.-K., Zhong, S.-L., Pei, J.-Y., Zhao, Y., Zhang, D.-L., Liu, D.-F., Zhang, Y.-X., and Dang, Z.-M. (2022). Recent Progress and Future Prospects on All-Organic Polymer Dielectrics for Energy Storage Capacitors. Chem. Rev. *122*, 3820–3878. 10.1021/acs.chemrev.1c00793.

60. Jiang, J., Shen, Z., Qian, J., Dan, Z., Guo, M., Lin, Y., Nan, C.-W., Chen, L., and Shen, Y. (2019). Ultrahigh discharge efficiency in multilayered polymer nanocomposites of high energy density. Energy Storage Mater. *18*, 213–221. 10.1016/j.ensm.2018.09.013.

61. Pan, Z., Li, L., Wang, L., Luo, G., Xu, X., Jin, F., Dong, J., Niu, Y., Sun, L., Guo, C., et al. (2023). Tailoring Poly(Styrene- *co* -maleic anhydride) Networks for All-Polymer Dielectrics Exhibiting Ultrahigh Energy Density and Charge–Discharge Efficiency at Elevated Temperatures. Adv. Mater. *35*, 2207580. 10.1002/adma.202207580.

62. Yuan, C., Zhou, Y., Zhu, Y., Liang, J., Wang, S., Peng, S., Li, Y., Cheng, S., Yang, M., Hu, J., et al. (2020). Polymer/molecular semiconductor all-organic composites for high-temperature dielectric energy storage. Nat. Commun. *11*, 3919. 10.1038/s41467-020-17760-x.